

On the Structural, Acidic and Catalytic Properties of Zeolite SUZ-4

Dmitri B. Lukyanov,^{*,||} Vladimir L. Zholobenko,^{†,‡} John Dwyer,[‡] Sami A. I. Barri,^{§,‡} and Warren J. Smith[∇]

UMIST Centre for Microporous Materials and Departments of Chemical Engineering and Chemistry, UMIST, P.O. Box 88, Manchester M60 1QD, U.K., and British Petroleum Chemicals, Research and Engineering, Sunbury on Thames, Middlesex TW16 7LL, U.K.

Received: August 24, 1998; In Final Form: November 2, 1998

Highly crystalline SUZ-4 zeolite was synthesized and its acidic and catalytic properties were investigated using FTIR spectroscopy and *n*-hexane conversion. Based on the analysis of the published crystallographic data, it is concluded that SUZ-4 zeolite has a three-dimensional pore system that includes ten-membered ring channels parallel to unit cell *c*-axis which are intersected by two arrays of eight-membered ring channels running in the plane [001]. Experimental results reported here support this conclusion. About 45% of acid sites (bridging hydroxyls) are located in the large channels of SUZ-4 zeolite, while the remaining sites occupy positions in nonplanar double eight-membered rings. The bridging hydroxyls in SUZ-4 zeolite are more accessible for guest molecules (*n*-hexane and isobutane) than those in ferrierite. Both zeolites show similar strength of acid sites and have similar protolytic cracking activity. The hydrogen transfer activity of ferrierite is observed to be higher than that of the SUZ-4 zeolite. These results indicate that SUZ-4 zeolite has potential as a catalyst and may display unusual shape-selective properties in comparison with other zeolites.

Introduction

SUZ-4 is a new synthetic zeolite patented by the British Petroleum Company.¹ XRD studies of this material show² that SUZ-4 framework topology is related to that of ferrierite which, in turn, is structurally related to the mineral wollastonite.^{2,3} The structure of ferrierite is well-known,⁴ and its two-dimensional pore system consists of ten-membered ring channels parallel to [001] interconnected with eight-membered ring channels parallel to [010]. Additionally, small channels formed by six-membered rings are present. Both the ten- and eight-membered ring channels in ferrierite are elliptical in shape with dimensions of 4.2 × 5.4 Å and 3.5 × 4.8 Å, respectively.⁴ The proposed² SUZ-4 framework consists of five-, six-, eight-, and ten-membered rings. According to Lawton et al.,² the pore system of this zeolite includes straight ten-membered ring channels and small cages linked through the double six-membered rings. The minimum and maximum dimensions of the ten-membered rings are 4.6 and 5.2 Å, respectively, which are very similar to those in ferrierite.

Consequently, on structural consideration, it might be expected that SUZ-4 zeolite would display catalytic properties similar to ferrierite which is reported⁵ to be an excellent catalyst for isomerization of *n*-butene into isobutene. However, the data published in ref 2 do not make immediately clear the nature of the channel system in SUZ-4. For instance, it is not evident from the representation given² whether this zeolite has a one-,

two-, or three-dimensional pore system. In addition, it appears that no information has yet been published on the acidic and catalytic properties of SUZ-4 zeolite.

The work described in this paper was undertaken in order to clarify acidic and catalytic properties of the new SUZ-4 zeolite in relation to its structure and to indicate the potential of this zeolite as a catalyst in hydrocarbon reactions. The results of a detailed FTIR characterization of acid sites in SUZ-4 zeolite in comparison with ferrierite are discussed in a different paper.⁶

Experimental Section

Materials. Two zeolites, namely, SUZ-4 and ferrierite, were used in this study. A template synthesized ferrierite was provided by BP Chemicals. Zeolite SUZ-4 was synthesized at UMIST according to the procedure described in the patent literature (ref 1b, example 6).

In a typical preparation, 3.5 g of potassium hydroxide and 2.0 g of sodium aluminate (BDH Grade; 40 wt % Al₂O₃, 30 wt % Na₂O, and the rest water) were dissolved in 75 g of distilled water. Tetraethylammonium hydroxide (5.0 g) solution (40 wt % in water) was then added to the solution followed by the addition of 20 g of Ludox AS40 colloidal silica (BDH Grade; 40 wt % SiO₂ in water). The resultant gel was stirred for 1 h and then heated in a revolving autoclave at 180 °C for 96 h. After this period, the product was removed from the autoclave and the content was filtered. The solid was washed with distilled water, dried overnight at 120 °C, and then calcined at 550 °C in air for 12 h. XRD analysis revealed the solid to be highly crystalline SUZ-4 zeolite (see Results and Discussion section). The chemical composition of the calcined SUZ-4 zeolite, expressed as a unit cell, was K_{4.6}Na_{0.4}Al_{5.0}Si_{31.0}O₇₂ (Si:Al = 6.2) which was very similar to that of the calcined ferrierite: K_{4.3}Na_{0.6}Al_{4.9}Si_{31.1}O₇₂ (Si:Al = 6.3). The NH₄-forms of SUZ-4 and ferrierite were obtained by contacting the calcined zeolite (4.0 g) with 1.0 M ammonium nitrate solution (80 mL) at 60

* To whom correspondence should be addressed at the Department of Chemical Engineering, UMIST, E-mail: MCDSTDBL@fs1.ch.umist.ac.uk, Fax: (44-161) 200-4399.

[†] Present address: Dept. of Chemistry, Keele University, Keele, Staffordshire ST5 5BG, UK.

[§] Present address: Dept. of Chemistry, KFUPM, P.O.Box 122, Dhahran 31261, Saudi Arabia.

^{||} Department of Chemical Engineering.

[‡] Department of Chemistry.

[∇] British Petroleum Chemicals.

°C for 2 h. After this, the solid was filtered and washed thoroughly with distilled water and the ion exchange procedure was repeated. Finally the zeolites were dried at 80 °C. Microanalysis indicated that the ion-exchange degree was 77% for SUZ-4 and more than 99% for ferrierite. It should be noted that after a single ion exchange the degree of ion-exchange in SUZ-4 zeolite was already about 75% and that an additional (third) ion exchange of the H,K-SUZ-4 sample with NH_4NO_3 solution did not change the residual content of potassium cations in the zeolite.

The following materials were used for catalytic and adsorption experiments: *n*-hexane (99.5+%) supplied by Fluka Chemika, oxygen (99.9%) and isobutane (99.5%) supplied by Messer Griesheim, and NH_3 (99.999%) obtained from Aldrich Chemical Co.

FTIR, XRD, NMR, and SEM Experiments. IR spectra of the self-supported zeolite disks were collected at a resolution of 2 cm^{-1} using a Nicolet Magna 550 FTIR spectrometer. Ammonia, *n*-hexane, and isobutane were used as test molecules to investigate acidic properties of the zeolites (number, strength, and accessibility of the acid sites). Adsorption of NH_3 was carried out at 150 °C, while *n*-hexane and isobutane were adsorbed at ambient temperature. Prior to all FTIR experiments the samples were calcined at 500 °C for 2 h in oxygen. The detailed experimental procedure is described elsewhere.^{6,7} XRD analysis of the zeolite powdered samples was carried out using a Philips 1710 diffractometer scanning at $1^\circ/\text{min}$ (2θ range from 5 to 40°). ^{27}Al MAS NMR spectra of the zeolite hydrated samples were obtained at room temperature employing a Bruker MSL 400 NMR spectrometer. $\text{Al}(\text{NO}_3)_3$ and TMS were used as references. Scanning electron microscopical (SEM) analysis of the NH_4 -forms of SUZ-4 and ferrierite samples was performed using a Philips SEM 525 microscope at the Manchester Materials Science Centre.

Catalysis. Catalytic properties of the zeolites were examined in the conversion of *n*-hexane at 400 °C. The reaction was carried out in a flow microreactor with a feed of 6.6 mol % *n*-hexane in N_2 . Protolytic cracking (PC) and hydrogen transfer (HT) activities of SUZ-4 zeolite were estimated and compared with those of ferrierite. The HT activity was determined following the procedure of the β -test^{8,9} based on the determination of the ratio between the rate of isobutane formation and concentration of isobutene in the reaction mixture at low (0–3%) conversions of *n*-hexane.

Results and Discussion

XRD, NMR, and SEM Studies. Powder X-ray diffraction data for calcined and ion-exchanged SUZ-4 samples were collected and compared with the published data.^{1b,2} The comparison indicated high crystallinity of the SUZ-4 zeolite prepared.

^{27}Al MAS NMR spectra of the hydrated SUZ-4 and ferrierite samples (NH_4 -forms) were recorded, and the only one peak, at about 56 ppm, attributed to tetrahedral Al in the zeolite framework, was observed. The absence of the extralattice Al (peak around 0 ppm) reflected retention of all Al atoms in the framework after calcination and ion exchange of the as-synthesized zeolites.

Scanning electron microscopy showed that the SUZ-4 crystallites had the shape of needles and rods with an average length and thickness of about 1.5 and 0.12 μm , respectively. The ferrierite crystallites could be described as platelets with an average diameter and thickness of about 1.0 and 0.1 μm , respectively. Aggregates of the ferrierite crystallites were smaller

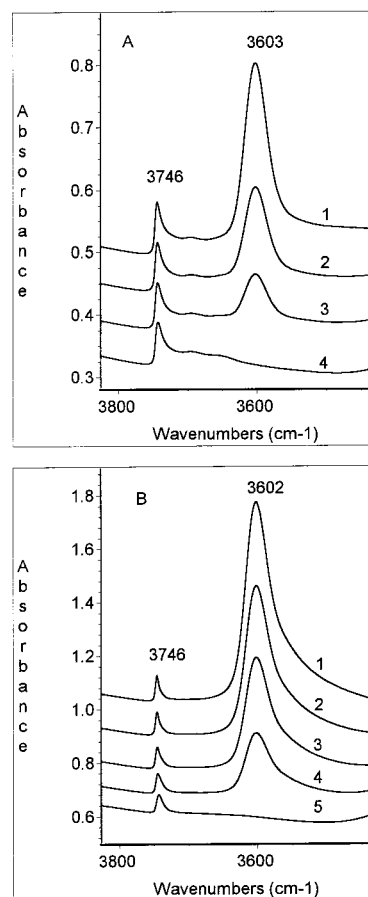


Figure 1. IR spectra (OH region) of H,K-SUZ-4 zeolite (A) and H-ferrierite (B) before (1) and after (2–5) NH_3 adsorption. Amount of NH_3 adsorbed (mmol/g) at 150 °C on SUZ-4 zeolite: 1–0; 2–0.55; 3–0.84; 4–1.34; on ferrierite: 1–0; 2–0.46; 3–0.89; 4–1.39; 5–2.04.

(on average) than aggregates of the SUZ-4 zeolite. Zeolite external surface areas were estimated to be 20.4 m^2/g for SUZ-4 sample and 14.1 m^2/g for ferrierite (the crystallites were considered as cylinders and a zeolite density of 1.7 g/cm^3 was used to calculate the surface area per gram of the zeolite).

FTIR Experiments. An IR spectrum (OH region) of the H,K-SUZ-4 zeolite (Figure 1A, spectrum 1) shows two bands at 3746 and 3603 cm^{-1} corresponding to terminal $\equiv\text{SiOH}$ groups and bridging hydroxyls ($\equiv\text{Al}(\text{OH})\text{Si}\equiv$), respectively. Only traces of hydroxyls associated with the extralattice Al species can be observed at $\sim 3688\text{ cm}^{-1}$, and this result is in good agreement with the ^{27}Al MAS NMR data. With ferrierite, only two bands at 3746 and 3602 cm^{-1} are observed in the IR spectrum (Figure 1B, spectrum 1).

The number, strength and accessibility of the acid sites in the H-forms of SUZ-4 zeolite and ferrierite were investigated by FTIR according to the procedure described earlier,⁷ using ammonia, *n*-hexane and isobutane as test molecules. Figure 1 shows the results of the experiments on ammonia adsorption carried out at 150 °C on H,K-SUZ-4 zeolite and H-ferrierite. Presented data demonstrate (i) that all bridging hydroxyls in both zeolites interact with NH_3 molecules ($\sigma = 2.6\text{ \AA}$)¹⁰ and (ii) that different numbers of these molecules are required to suppress completely the IR bands, corresponding to these hydroxyls, in the two zeolites studied. At the same time, Figure 1 indicates that most of the SiOH groups and OH groups, associated with the extralattice Al species, do not interact with NH_3 . Therefore, the amount of NH_3 adsorbed was used to determine the number of acid sites in the zeolites and was found

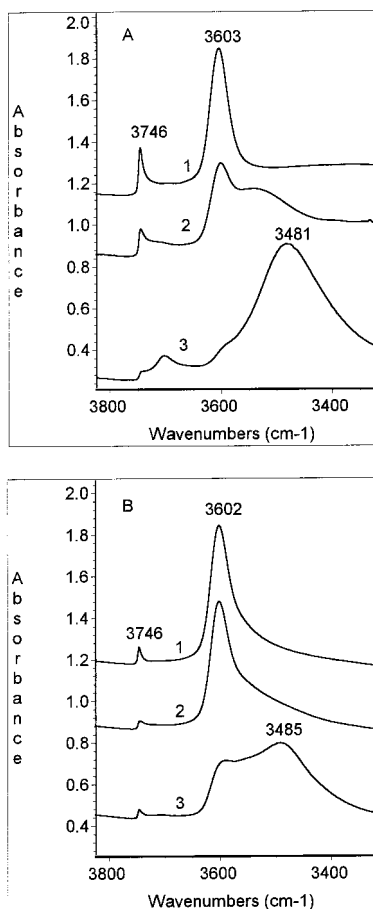


Figure 2. IR spectra (OH region) of H,K-SUZ-4 zeolite (A) and H-ferrierite (B) before (1) and after adsorption of isobutane (2) or *n*-hexane (3).

to be 10.2×10^{20} sites/g for SUZ-4 zeolite and 11.8×10^{20} sites/g for ferrierite. These numbers are in good agreement with the estimates based on chemical analysis (9.5×10^{20} and 12.1×10^{20} acid sites/g for SUZ-4 and ferrierite, respectively). It should be noted that the amount of acid sites in SUZ-4 is lower than that in ferrierite, since the SUZ-4 zeolite contains a considerable amount ($\sim 23\%$) of nonexchangeable potassium cations, while ferrierite sample is fully ion exchanged (see Experimental Section).

To estimate the acid strength of the accessible bridging OH groups in SUZ-4 and ferrierite the adsorption of *n*-hexane on these zeolites was studied at ambient temperature. In these experiments the *n*-hexane pressure was increased stepwise and the IR spectra collected after each step. Figure 2A (spectrum 3) presents the final spectrum which showed no further change in intensity on increase in *n*-hexane pressure. The shift of the band corresponding to the acidic OH group interacting with *n*-hexane was measured and used as a qualitative estimate of the acidity of the OH groups. Figure 2A (bands at 3481 and 3603 cm^{-1}) shows that this shift is about 122 cm^{-1} in the case of SUZ-4 zeolite, while it is around 117 cm^{-1} for ferrierite (see Figure 2B, bands at 3485 and 3602 cm^{-1}). These data suggest that the bridging hydroxyls in the H,K-SUZ-4 zeolite and H-ferrierite are of the similar acidity, and this suggestion is further supported by NH_3 TPD experiments.⁶

The *n*-hexane adsorption data were also used to estimate the number of the acid sites accessible to *n*-hexane in SUZ-4 zeolite and ferrierite. Difference IR spectra were used to obtain quantitative estimates, and the intensity of the negative band at $\sim 3603 \text{ cm}^{-1}$ (corresponding to loss of OH groups due to

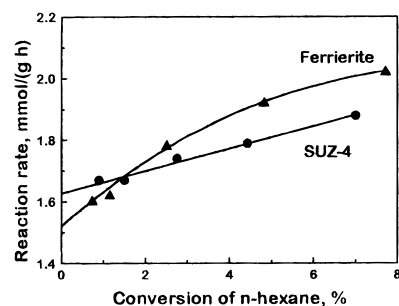


Figure 3. Rates of *n*-hexane transformation as functions of *n*-hexane conversion over H,K-SUZ-4 zeolite and H-ferrierite at 400 °C.

interaction with *n*-hexane) was measured and compared to the initial band intensity. The same procedure was applied to estimate the accessibility of the acid sites for isobutane.

Investigation of SUZ-4 zeolite revealed that about 97 and 44% of acid sites are accessible for *n*-hexane and isobutane, respectively. The corresponding values for ferrierite were found to be about 70 and 23%. These results, illustrated by the data in Figure 2A (SUZ-4 zeolite) and Figure 2B (ferrierite), indicate clearly that the acid site accessibility in H,K-SUZ-4 zeolite is higher for both *n*-hexane and isobutane than that in ferrierite, and consequently, the pore system of H,K-SUZ-4 zeolite appears to be more open for guest molecules ($n\text{C}_6$ and $i\text{C}_4$) than the pore system of ferrierite. However, it should be emphasized that both zeolites demonstrate similarity in the adsorption behavior with *n*-hexane and isobutane, since for both zeolites the acid site accessibility for isobutane, $\sigma = 5.0 \text{ \AA}$,¹⁰ is significantly lower than that observed for *n*-hexane, $\sigma = 4.3 \text{ \AA}$.¹⁰ In the case of ferrierite this fact can be easily explained, since this zeolite has ten- and eight-membered ring channels, and the acid sites located in the smaller channels cannot be reached by isobutane. In the case of SUZ-4 zeolite only the ten-membered ring channels were emphasized previously.² Our data suggest strongly that the other channels, namely, eight-membered ring channels, which are evident in a structural or computational model based on the coordinates given in ref 2, are also present in SUZ-4. The acid sites located in these eight-membered ring channels are not accessible for isobutane molecules and this explains the difference in the acid site accessibility for *n*-hexane and isobutane that is observed in the experiments with SUZ-4 zeolite. It should be noted that the detailed FTIR investigation of the acid sites in this zeolite has demonstrated⁶ existence of two overlapping IR bands at 3592 and 3610 cm^{-1} (of high similar intensity) which were assigned to the bridging OH groups in the eight- and ten-membered rings, respectively.

Catalysis. Catalytic properties of SUZ-4 zeolite and ferrierite were compared in conversion of *n*-hexane. Figure 3 shows that at 400 °C the rate of *n*-hexane transformation increases with conversion. The observed autocatalytic effect is in agreement with previous investigations of this reaction at low temperatures (350–400 °C),^{11,12a} and can be explained by existence of two reaction mechanisms.¹² Mechanism A involves monomolecular protolytic cracking (PC) of *n*-hexane on acid sites resulting in formation of hydrogen and C_1 – C_4 product paraffins (and corresponding olefins). Mechanism B involves bimolecular hydrogen transfer (HT) steps between *n*-hexane and carbenium ions, formed by product olefins, and results, mainly, in formation of C_3 , $n\text{-C}_4$, and $i\text{-C}_4$ paraffins. Figures 4 and 5 illustrate clearly the operation of these two mechanisms in *n*-hexane conversion over SUZ-4 zeolite and ferrierite, respectively. The rates of

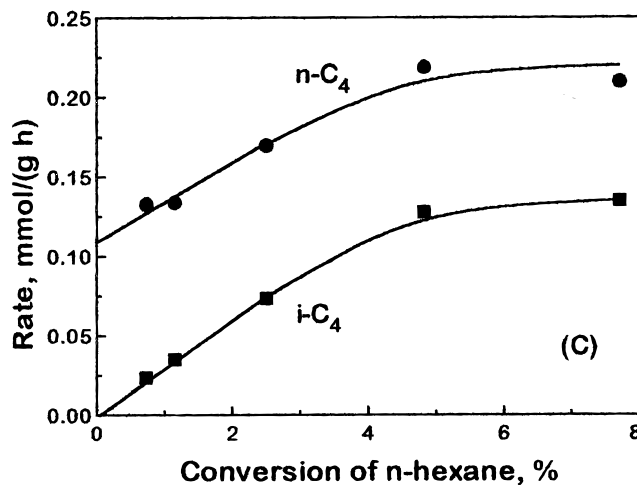
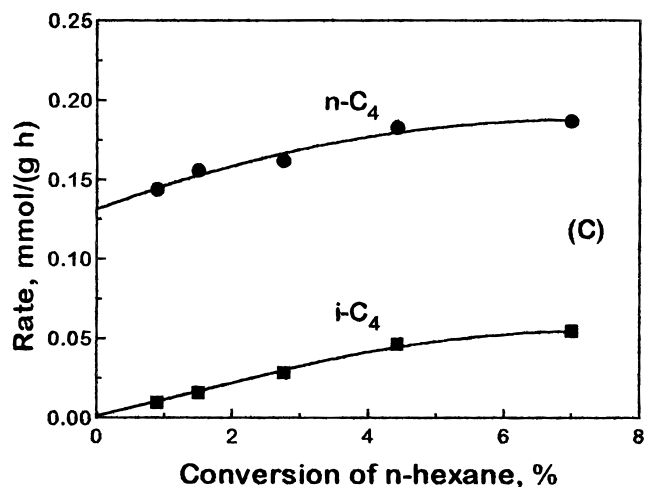
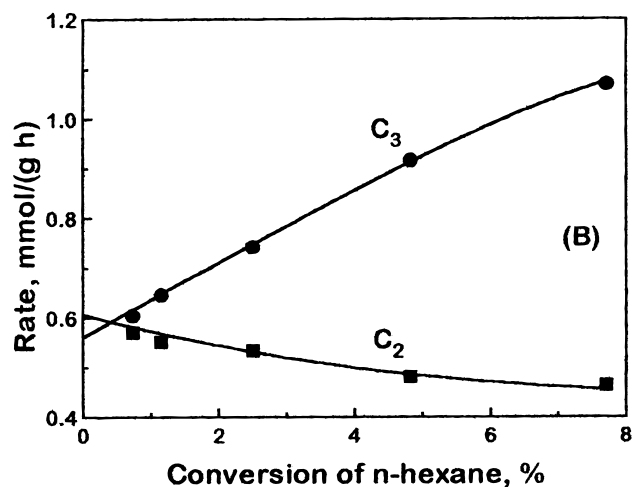
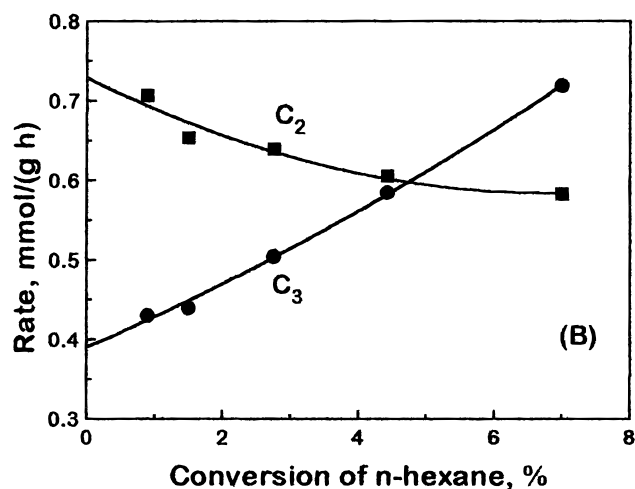
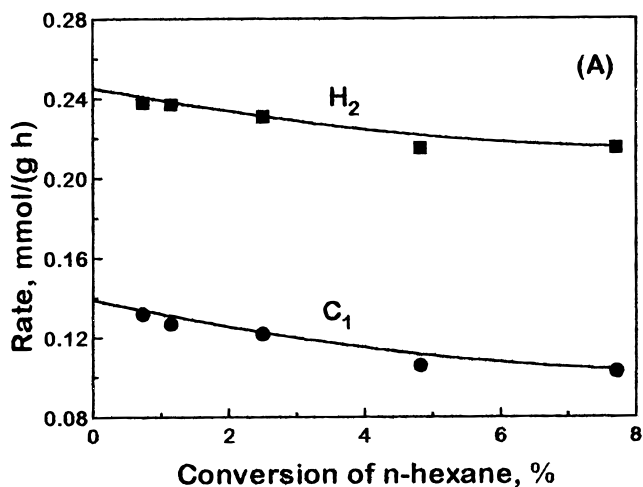
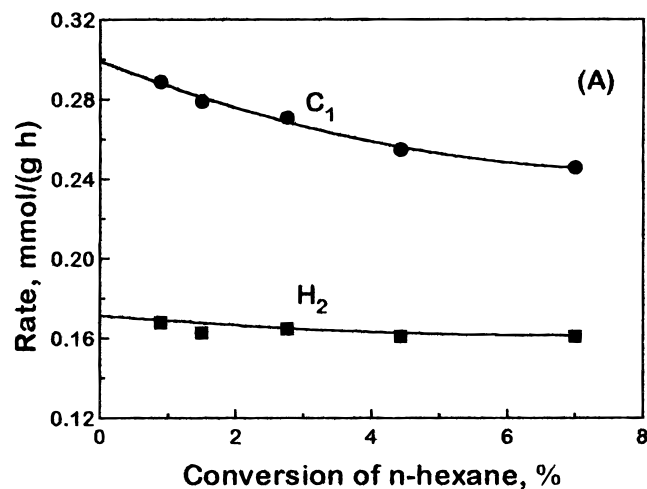


Figure 4. Rates of formation of H₂ and C₁–C₄ product paraffins as functions of *n*-hexane conversion over H,K-SUZ-4 zeolite at 400 °C.

formation of hydrogen, methane and ethane decrease with increasing *n*-hexane conversion indicating that these products are formed via mechanism A only. On the contrary, the rates of formation of propane and *n*-butane increase with the conversion due to additional formation of these paraffins in the hydrogen transfer steps of the reaction (mechanism B). Isobutane, which is not a primary product of the reaction, is formed via mechanism B only.^{8,9,12} Consequently, the rate of isobutane formation is zero at zero *n*-hexane conversion and increases with increasing conversion level (see Figures 4C and 5C).

Figure 5. Rates of formation of H₂ and C₁–C₄ product paraffins as functions of *n*-hexane conversion over H-ferrierite at 400 °C.

Protolytic cracking activities of SUZ-4 zeolite and ferrierite were estimated by extrapolation of the experimental data shown in Figure 3 to zero conversion of *n*-hexane. The estimates obtained (see Table 1) show that catalytic sites in the two zeolites are of similar activity. This finding is in accordance with the above conclusion on the strength of the acid sites in these zeolites as determined by FTIR.

Hydrogen transfer activities of the two zeolites were estimated following the procedure of the β -test,⁸ which is based on determination of the ratio between the rate of isobutane

TABLE 1: Protolytic Cracking (PC) and Hydrogen Transfer (HT) Activities of SUZ-4 Zeolite and Ferrierite in Conversion of *n*-Hexane at 400 °C

zeolite	PC activity, mmol/(g h)	PC activity, ^a molecule/(site h)	HT activity, mmol/(g h atm)	HT activity, ^a molecule/(site h atm)
SUZ-4	1.64	0.97	120	71
ferrierite	1.55	0.79	530	270

^a PC and HT activities per active site were calculated based on the numbers of acid sites estimated from NH₃ adsorption (see text).

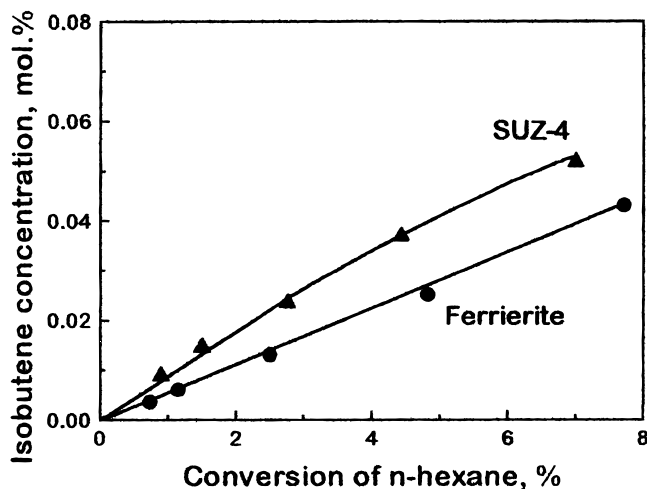


Figure 6. Isobutene concentrations as functions of *n*-hexane conversion over H,K-SUZ-4 zeolite and H-ferrierite at 400 °C.

formation ($R(iC_4)$) and the isobutene concentration in gas phase ($[iC_4^-]$). With a number of different zeolites and at low *n*-hexane conversions, this ratio has been found to be a constant which is proportional to the rate constant of the hydride transfer step between *n*-hexane and a *tert*-butyl carbenium ion.^{8,9} Thus, the $R(iC_4)/[iC_4^-]$ ratio can be used for quantitative characterization of the HT activity of zeolite catalysts. The experimental results obtained in this study show that both the isobutane formation rate (Figures 4C and 5C) and the isobutene concentration (Figure 6) are strictly proportional to *n*-hexane conversion up to conversions around 2.5%. Hence, the $R(iC_4)/[iC_4^-]$ ratio is constant for each catalyst and has been used to estimate quantitatively the HT activities of these two catalysts. The estimates obtained are shown in Table 1 and clearly demonstrate that ferrierite is about 4 times more active in the bimolecular hydrogen transfer reaction than SUZ-4 zeolite. Such a difference results in the different rate enhancement with increasing *n*-hexane conversion over the two zeolites (Figure 3) and may be due to differences in proximity of acid sites¹³ and/or different local spacial restrictions (formation of a bulky transition state is required for hydrogen transfer reactions)^{9,14} in SUZ-4 zeolite and ferrierite. At this time we are not able to make final discrimination between these features, although the results on isobutane adsorption in SUZ-4 and ferrierite as well as consideration of the structures of these two zeolites (given below) suggest that the local spacial factor may not be responsible for reduced hydrogen transfer in SUZ-4 zeolite. This may imply that the hydrogen transfer in SUZ-4 zeolite and ferrierite is influenced by differences in Al distribution in these zeolites. This point is further supported by the investigation of the mesitylene isomerization reaction which can proceed only on the acid sites located on the external surface of the zeolite crystallites. This study was carried out at 400 °C, and the results obtained demonstrated¹⁵ that the ferrierite was about 6 times more active in this reaction in comparison with the SUZ-4

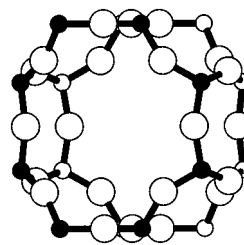


Figure 7. Nonplanar double eight-membered ring in SUZ-4 zeolite. "T" atoms: ●, in front ring; ○, in back ring.

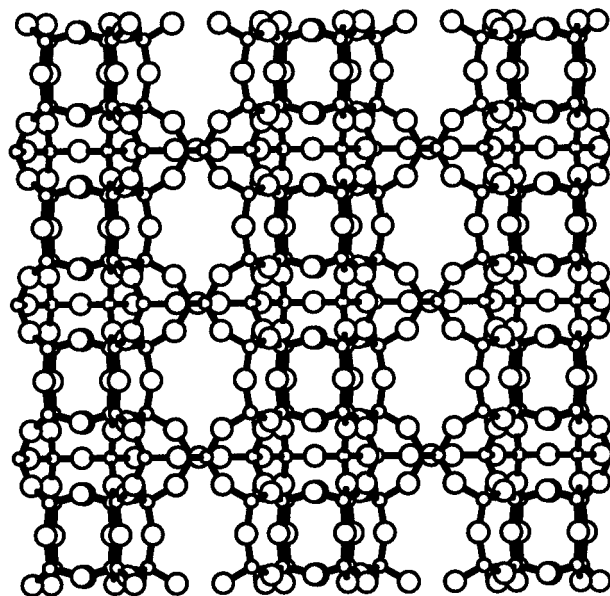


Figure 8. SUZ-4 zeolite viewed along eight-membered ring channels.

zeolite. This finding, taken together with the data on the external surfaces of the both zeolites (20.4 and 14.1 m²/g for SUZ-4 and ferrierite, respectively), clearly indicate the differences in Al distribution in the crystallites of the two zeolites and suggest that the local Al distribution (and, consequently, the local site densities) may be considerably different in these zeolites. In conclusion of this part of the paper, we would like to note that the HT activity of the ferrierite (per gram) was found to be about 3 times lower than the corresponding activity of HZSM-5 zeolite (Si:Al = 17). This fact is probably not surprising, since the local spacial restrictions in ferrierite should be much more stronger in comparison with those in HZSM-5.

SUZ-4 Channel System. To investigate topology of the eight-membered ring channels in the SUZ-4 zeolite, we used the published structural data² to model the framework of this zeolite. This modeling revealed that the nonplanar double eight-membered rings (Figure 7), previously reported² to exist in SUZ-4, actually form two eight-membered ring channels which intersect the straight ten-membered ring channel described by Lawton et al.² The angle between the former two channels is about 74° and they are in the plane [001], perpendicular to the direction of the ten-membered ring channels. The view along the eight-membered ring channels, which is the same for both of them, is shown in Figure 8, and the schematic representation of the multichannel system in the SUZ-4 zeolite is given in Figure 9.

Thus, analysis of the published structural data shows that the new SUZ-4 zeolite should be regarded as having a three-dimensional pore system, while the channel system in ferrierite is two-dimensional. Presumably, this difference may explain why the acid sites in H,K-SUZ-4 zeolite are more accessible

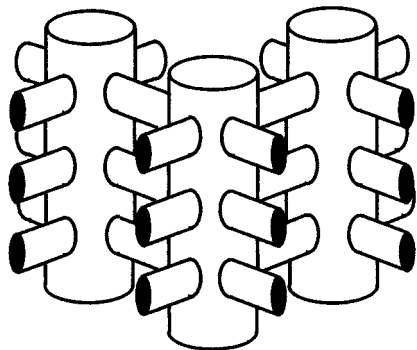


Figure 9. Schematic representation of the SUZ-4 multichannel system.

to *n*-hexane molecules than those in H-ferrierite. On the basis of the FTIR and structural studies of H,K-SUZ-4 zeolite, it is suggested that about 45% of the acid sites are located in the straight ten-membered ring channels, while the remaining sites occupy positions in the double eight-membered rings shown in Figure 7, and that both sites are accessible to *n*-hexane. It seems likely that the nonexchangeable potassium cations in H,K-SUZ-4 zeolite can be concentrated in small cages² and/or in double six-membered rings which are present in SUZ-4 zeolite but not in ferrierite.

Conclusions

The pore system of the new zeolite SUZ-4 is formed by the intersecting ten- and eight-membered ring channels and should be considered as three-dimensional. The acid sites in SUZ-4 zeolite are more accessible for *n*-hexane and isobutane than sites in ferrierite. However, the bridging hydroxyls in both zeolites are similar in acidity and display similar protolytic cracking activity in the conversion of *n*-hexane. On the other hand, the hydrogen transfer activity of ferrierite is found to be higher than that of the SUZ-4 zeolite (possibly, because of the different Al distribution in these two zeolites). Thus, our results indicate that the new SUZ-4 zeolite has potential as a catalyst which may display unusual shape-selective properties in comparison with other zeolites.

Acknowledgment. We thank Dr. A. A. Garforth and Mrs. T. G. Vajnova for general experimental assistance and Dr. S. M. Holmes for XRD analysis. Also, we thank BP Chemicals for financial support and permission for this publication. We gratefully acknowledge the EPSRC for Grant GR/K44305 for V.L.Z. and for the equipment grant, Grant GR/L24908.

References and Notes

- (1) (a) Barri, S. A. I. (British Petroleum Company (GB)). U.S. Patent 5 118 483, 1992. (b) Barri, S. A. I. (British Petroleum Company (GB)). European Patent 0353915, 1994.
- (2) Lawton, S. L.; Bennett, J. M.; Schlenker, J. L.; Rubin, M. K. *J. Chem. Soc., Chem. Commun.* **1993**, 894.
- (3) Gramlick-Meier, R. *Z. Kristallogr.* **1986**, *177*, 237.
- (4) Meier, W. M.; Olson, D. H.; Baerlocher, Ch. *Atlas of Zeolite Structure Types*, 4th revised ed.; Elsevier: London, 1996; p 106.
- (5) (a) Grandvallet, P.; Mooiweer, H. H.; Kortbeek, A. G. T.; Kraushaar-Czarnetzki, B. (Shell International (Netherlands)). European Patent 0501577A1, 1992. (b) Mooiweer, H. H.; de Jong, K. P.; Kraushaar-Czarnetzki, B.; Stork, W. H. J.; Krutzen, B. C. H. *Stud. Surf. Sci. Catal.* **1994**, *84*, 2327.
- (6) Zholobenko, V. L.; Lukyanov, D. B.; Dwyer, J.; Smith, W. J. *J. Phys. Chem. B* **1998**, *102*, 2715.
- (7) Zholobenko, V. L.; Makarova, M. A.; Dwyer, J. *J. Phys. Chem.* **1993**, *97*, 5962.
- (8) Lukyanov, D. B. *J. Catal.* **1994**, *145*, 54.
- (9) Lukyanov, D. B. *J. Catal.* **1994**, *147*, 494.
- (10) Breck, D. W. *Zeolite Molecular Sieves*; John Wiley & Sons: New York, 1974; pp 636, 637.
- (11) Lukyanov, D. B.; Shtral, V. I.; Khadzhev, S. N. *J. Catal.* **1994**, *146*, 87.
- (12) (a) Haag, W. O.; Dessau, R. M. In *Proceedings of the 8th International Congress on Catalysis*, Berlin, 1984; Dechema, Berlin, 1984; Vol. 2, p 305. (b) Corma, A.; Planelles, J.; Sanchez-Marin, J.; Thomas, F. *J. Catal.* **1985**, *93*, 30.
- (13) (a) Pine, L. A.; Maher, P. J.; Wachter, W. A. *J. Catal.* **1984**, *85*, 466. (b) Giannetto, G.; Sansare, S.; Guisnet, M. *J. Chem. Soc., Chem. Commun.* **1986**, 1302. (c) Corma, A.; Faraldos, M.; Martinez, A.; Mifsud, A. *J. Catal.* **1990**, *122*, 230. (d) Wielers, A. F. H.; Vaarkamp, M.; Post, M. F. M. *J. Catal.* **1991**, *127*, 51.
- (14) (a) Haag, W. O.; Lago, R. M.; Weisz, P. B. *Faraday Discuss. Chem. Soc.* **1982**, *72*, 317. (b) Chen, N. Y.; Haag, W. O. *Hydrogen Effects in Catalysis. Fundamentals and Practical Applications*; Paal, Z., Menon, P. G., Eds.; Dekker: New York, 1988; p 695.
- (15) Lukyanov, D. B.; Vajnova, T. G. Unpublished results.